Accepted Manuscript

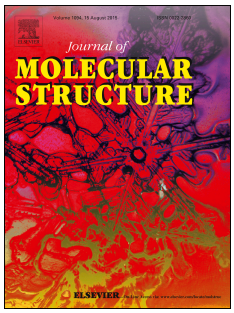

Chemical synthesis, spectroscopic studies, chemical reactivity properties and bioactivity scores of an azepin-based molecule

Shiva Prasad Kollur, Joaquín Ortega Castro, Juan Frau, Daniel Glossman-Mitnik

PII: S0022-2860(18)31374-7

DOI: https://doi.org/10.1016/j.molstruc.2018.11.061

Reference: MOLSTR 25890

To appear in: *Journal of Molecular Structure*

Received Date: 17 October 2018

Revised Date: 21 November 2018

Accepted Date: 21 November 2018

Please cite this article as: S.P. Kollur, Joaquí.Ortega. Castro, J. Frau, D. Glossman-Mitnik, Chemical synthesis, spectroscopic studies, chemical reactivity properties and bioactivity scores of an azepin-based molecule, *Journal of Molecular Structure* (2019), doi: https://doi.org/10.1016/j.molstruc.2018.11.061.

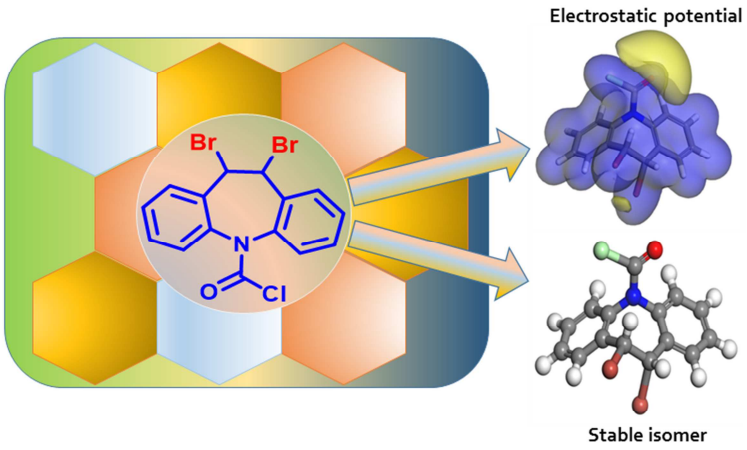

Chemical Synthesis, Spectroscopic Studies, Chemical Reactivity Properties and Bioactivity Scores of an Azepin-based Molecule

Shiva Prasad Kollur[a,*], Joaquín Ortega Castro[b], Juan Frau[b], Daniel Glossman-Mitnik[b,c]

[a]*Chemistry Group, Manipal Centre for Natural Sciences, Manipal Academy of Higher Education, Manipal - 576 104, Karnataka, India*

[b]*Departament de Química, Universitat de les Illes Balears, Palma de Mallorca 07122, Spain*

[c]*Laboratorio Virtual NANOCOSMOS, Departamento de Medio Ambiente y Energía, Centro de Investigación en Materiales Avanzados, Miguel de Cervantes 120, Complejo Industrial Chihuahua, Chihuahua, Chih 31136, Mexico*

[*]Corresponding author

Email address: shivachemist@gmail.com (Shiva Prasad Kollur)

Abstract

Azepines derived molecules are of great interest because of their multi-drug like properties and thus advantageous in biomedical field. Herein, a novel route is described for the synthesis of an azepine-based molecule, 10,11-Dibromo-10,11-dihydro- 5H-dibenzo[b,f]azepine-5-carbonyl chloride (DACC) by using dibutyltin dilaurate (DBTDL) as catalyst. The structure of DACC was elucidated by using FT-IR, NMR, and mass spectroscopic techniques. Several density functionals were considered for the study of the molecular properties of the synthesized compound. The global and local reactivity descriptors were estimated by using Conceptual Density Functional Theory (CDFT). The active sites suitable for the nucleophilic and electrophilic attacks were selected by linking them with the Fukui indices, Parr functions and condensed Dual Descriptor Δ f(r). Finally, the bioactivity scores for the studied molecule were predicted through different methodologies.

Keywords: Azepine, Spectroscopy, Conceptual DFT, Reactivity Descriptors, Biological Scores

Introduction

The tricyclic heterocycles presented in Figure 1, Iminostilbene (1) and its azepine derivatives (2, 3) are well-known anticonvulsants and CNS-active drugs widely used in the treatment of various disorder such as acute mania, trigeminal neuralgia and epilepsy [1], as they possess important pharmacological activities [2–4]. Thus, the synthesis of benzoazepines analogues is a continuous task of research and development and a standout amongst the active areas in synthetic chemistry [5].

Figure 1: Iminostilbene (1) and its azepine derivatives Oxcarbazepine (2) and Carbamazepine (3).

One of the objectives of the present work is to present a novel route for the synthesis of a bromo derivative of an azepine-based molecule, namely Carbamazepine. This derivative whose IUPAC name is 10,11-dibromo-10,11-dihydro-5H-dibenzo[b,f] azepine-5-carbonyl chloride will be characterized by experimental and theoretical FT-IR and UV-Vis spectra. Recently, the synthesis of 11-methoxy-6,6a-dihydro- 5H-dibenzo[b,e]azepine and its spatial conformation has been reported, which was compared with the X-ray crystal structure data of similar molecule and theoretically predicted its biological activity based HOMO-LUMO energy values [6]. Moreover, as the bioactivity properties of these kind of compounds are closely related to their chemical reactivity [7, 8], a study of these properties will be performed by resorting to Density Functional Theory (DFT) as well as Conceptual DFT which is a powerful tool for the prediction, analysis and interpretation of the outcome of chemical reactions [9–12]. Further, the weak interactions within the polyaromatic π-molecular systems are influences of the properties of molecule which can be determined rationally with aid of DFT calculations in addition to HOMO-LUMO energy values, that will further reflect the bioactivity of the molecule [13, 14]. At last, the descriptors of bioavailability and bioactivity which are called Bioactivity Scores will be figured through various methodologies effectively depicted in recent publications [15, 16].

Experimental Section

All chemicals were obtained from Sigma Aldrich (USA) and the solvents were of AR grade, obtained from Merck chemical company (India). Solvents were distilled by known procedures before use. Infrared spectra was measured using Perkin-Elmer Spectrometer version 10.03.09. The UV-Visible absorption spectra was measured using UV1800 UV-Visible spectrophotometer (Shimadzu). ^{1}H and ^{13}C-NMR spectra were recorded on Bruker 400 MHz NMR spectrometer with TMS as internal standard. The compound was dissolved in the $CDCl_3$. Chemical shifts are expressed in parts per million (ppm). The mass spectrum of the compound(s) was obtained by TOF-ES technique at 70 eV using ESI/APCI-hybrid mass spectrometer (Waters, USA).

Theoretical Background and Computational Details

The molecular structure of the DACC molecule was drawn from scratch by using the MarvinSketch 17.15 program (https://www. chemaxon.com). A preoptimization was performed by selecting the most stable conformers, a task which was accomplished by means of Molecular Mechanics techniques with the inclusion of the various torsional angles via the general MMFF94 force field [17–21] involving the MarvinView 17.15 program. The lowest energy conformation for each molecule was chosen to calculate the electronic energy and the Highest Occupied Molecular Orbital (HOMO) and the Lowest Occupied Molecular Orbital (LUMO) at the DFT functional levels mentioned in the next paragraph. On the basis of the experience adcquired with similar calculations on melanoidins [22–28] and peptides of marine origin [29], the computational studies were performed with Gaussian 09 [30] using the Def2TZVP basis set for the geometry optimization and frequency determination as well as for the calculation of the electronic properties [31, 32]. All calculations were performed in the presence of chloroform as solvent under the Solvation Model Density (SMD) parameterization of the Integral Equation Formalism-Polarized Continuum Model (IEF-PCM) [33]. To calculate the molecular structure and properties of the studied systems, we have chosen several density functionals: B3LYP [34], BLYP [35, 36], PBE0 [37], PBEPBE [38, 39], CAM-B3LYP [40], M11 [41], M11L [42], MN12L [43], MN12SX [44], N12 [45], N12SX [44], HSEH1PBE [46–52] and ωB97XD [53].

The SMILES notation of the studied compound was fed in the online Molinspiration software from Molinspiration Cheminformatics (www.molinspiration.com) for the calculation of the molecular properties (Log P, Total polar surface area, number of hydrogen bond donors and acceptors, molecular weight, number of atoms, number of rotatable bonds, etc.) and for the prediction of the bioactivity score for different drug targets (GPCR ligands, Kinase inhibitors, Ion channel modulators, Enzymes and Nuclear receptors). The bioactivity scores were compared with those obtained through the use of other software like MolSoft from Molsoft L.L.C. (http://molsoft.com/mprop/) and ChemDoodle Version 9.02 from iChemLabs L.L.C. (www.chemdoodle.com).

Results and Discussion

The synthesis of DACC (**5**) was achieved following the scheme displayed in Figure 2 by reacting 1H-indole (1) (1.5 mM in 15 mL toluene) with aryl bromide (2.0 mM in 10 mL toluene) in presence of dibutyltin dilaurate (DBTDL) as catalyst and continuously stirred and refluxed for 12 h to yield compound **2**. To the solution of compound **2** (1.2 mM in 10 mL toluene), a mixture of P_2O_5-CH_3SO_3H (1:10) was added drop wise with stirring and heated to reflux for 6 h at 120 $^{\circ}$C. The synthesis of compound **4** was achieved by treating compound **3** (1.5 mM in 15 mL toluene) with triphosgene (0.3 mM in 15 mL toluene) and reflux for 2.5 h under nitrogen atmosphere to afford a pale yellow solid. Finally, the target compound **5** was synthesized by reacting compound **4** (1.25 mM) with NBS (4.45 mM) in methanol as reported previously [54]. The completion of reaction was monitored by thin layer chromatography and spots were visualized under UV light.

Figure 2: Synthesis of 10,11-Dibromo-10,11-dihydro-5H-dibenzo[b,f]azepine-5-carbonyl chloride (5) starting from 1H-indole.

The structure of synthesized compound was characterized using FT-IR, NMR and mass spectral techniques. The detailed spectral characterization for DACC molecule is given in the synthesis

section. The FT-IR spectrum showing characteristic band at 3299 cm^{-1} is ascribed to aromatic C-H stretching; and sharp bands, observed between 1382-1326 cm^{-1} indicates the presence of C-N stretch. The presence of carbonyl stretch was confirmed by observing sharp band at 1797 cm^{-1}. The molecular structure was further confirmed by ^{1}H and ^{13}C NMR spectral analysis. A singlet peak observed at 3.86 ppm was attributed to methyl protons of N-CH_3 group and another singlet peak observed at 2.48 ppm was ascribed for protons of methyl group attached directly to aromatic ring. A triplet peak between 0.87-0.78 ppm was assigned to free methyl protons of aromatic propyl moiety. Similarly, a sextet and a triplet observed between 1.78-1.66 and 2.72-2.69 ppm were due to two methylene group protons under different environment in aromatic propyl group, respectively. The aromatic protons were seen around 7.29-7.77 ppm region. In support to this, ^{13}C NMR spectral data also revealed the presence of imidazole rings at 157.30 and 155.34 ppm. Further appearance of the molecular ion peak at 305.17 (M + 1) confirmed the structure of DACC.

The molecular structure of the conformers of the DACC molecule were acquired as specified in the Computational Details section and were optimized again by using the DFTBA subprogram accessible in Gaussian 09 and after that optimized once more utilizing the previously mentioned density functionals together with Def2TZVP as the basis set and the SMD model with chloroform as the solvent. Subsequent to checking that every one of the structures were related to the minimum energy conformations through a frequency calculation analysis, the electronic properties, in particular the electronic energy and the energies of the HOMO and LUMO, were calculated by utilizing a similar model at the same level of theory than that utilized for the geometry optimization.

It is standard to check if the utilized density functionals permit to obtain results distinguishing the energy of the HOMO with the Ionization potential of the neutral species, I, also the energy of the LUMO with the Electron Affinity of a similar framework, A, on the grounds that this would make it simpler to anticipate the Conceptual DFT descriptors of the compound reactivity. Previously, a concurrent technique alluded to as the ”KID procedure”, attributable to its correspondences with the Koopmans’ theorem, was proposed by the some of the authors [22–29]. As it has been clarified in the last referenced works, KID remains for ”Koopmans in DFT” and is a method to check the confirmation of the ϵ_H (N) = -IP(N) fulfillment and in the meantime an examination between the ϵ_L (N) of the neutral (the LUMO) and the estimation of A for a similar system [22–29]. . The investigation of the outcomes got in the examination went for checking that the KID methodology was satisfied. On doing it beforehand, some descriptors related with the outcomes that the HOMO and LUMO computations got are connected with results got utilizing the vertical I and A following the Δ SCF method. A connection exists between the three fundamental descriptors and the most straightforward adjustment to the Koopmans’ hypothesis by connecting ϵ_H with -I, ϵ_L with -A, and their behavior in describing the HOMO–LUMO gap as $J_I = |\epsilon_H + E_{gs}(N-1) - E_{gs}(N)|$, $J_A = |\epsilon_L + E_{gs}(N) - E_{gs}(N+1)|$, and $J_{HL} = \sqrt{J_I^2 + J_A^2}$ [22–29]. The results of this investigation are exhibited in Table 1.

Table 1: Electronic energies of the neutral, positive, and negative molecular systems (in au) of the DACC molecule; the HOMO and LUMO orbital energies (in eV); and the J_I, J_A, and J_{HL} descriptors calculated as mentioned in the text.

Density Functional	Eo	E+	E-	HOMO	LUMO	J_I	J_A	J_{HL}
B3LYP	-6316.48	-6316.21	-6316.55	-7.05	-2.06	0.008	0.009	0.012
BLYP	-6316.2	-6315.9	-6316.2	-6.04	-2.90	0.078	0.029	0.083

	0	5	8					
PBE0	-6314.85	-6314.58	-6314.91	-7.23	-1.60	0.002	0.003	0.003
PBEPBE	-6314.59	-6314.34	-6314.66	-6.19	-2.73	0.027	0.028	0.039
CAM-B3LYP	-6316.31	-6316.03	-6316.36	-8.45	-0.53	0.037	0.030	0.048
M11	-6315.44	-6315.15	-6315.48	-9.51	0.27	0.069	0.059	0.091
M11L	-6316.22	-6315.96	-6316.29	-6.60	-2.59	0.025	0.025	0.036
MN12L	-6313.51	-6313.25	-6313.56	-6.39	-2.00	0.025	0.024	0.034
MN12SX	-6314.58	-6314.31	-6314.63	-6.95	-1.94	0.015	0.016	0.022
N12	-6319.44	-6319.19	-6319.49	-6.03	-2.36	0.027	0.028	0.038
N12SX	-6312.10	-6311.83	-6312.15	-6.79	-1.88	0.015	0.016	0.022
HSEH1PBE	-6314.89	-6314.62	-6314.95	-6.85	-2.00	0.015	0.015	0.022
ωB97XD	-6316.30	-6316.03	-6316.34	-8.98	0.14	0.058	0.051	0.077

An inspection of Table 1 reveals that the results for the J_I, J_A and J_{HL} descriptors are very close to zero and this means that they follow the KID procedure well. It can be thought that it is not possible to discriminate between the different density functionals to chose those which are well-behaved for the description of the electronic properties. However, it can be also appreciated from Table 1 that the values of the energy of the LUMO for the M11 and the ωB97XD density functionals is positive which implies that in the realm of the Koopmans approximation their Electron Affinity A will be negative, which is an unphysical result. Thus, both functionals may be omitted from the present study.

For the remaining density functionals it will be necessary to perform a comparison with the results of an experimental observation, for example how well they predict the absorption spectrum and that will accomplished next.

The experimental absorption spectrum of the DACC molecule in $CHCl_3$ is displayed in Figure 3. It can be seen that there are two prominent peaks: one is located at 270 nm and belongs to the

convolution of different excitations of similar energy; the other belongs to the HOMO-LUMO transition at it is located at 353 nm.

Figure 3: Experimental absorption spectrum of DACC in $CHCl_3$

The usual way to predict the absorption spectrum through calculations is by performing a Time-Dependent Density Functional Theory (TDDFT) study at the geometry of the optimized molecular structure. The direct calculation is called Linear Response (LR) TDDFT and it usually presented in this way in most of the studies. The other way to perform the calculations is appropriate for modeling solvation effects on dark absorptions (excitations with relatively small oscillator strengths). For these cases, the LR approach would not recover the solvation effects on the absorption energies. Instead, it is necessary to perform a more complex, two-part solvation study which is called state-specific (SS) because it refers to a calculation which focuses on modeling the properties of a specific excited state [55]. Moreover, an approximate prediction of the maximum absorption wavelength can be made by considering the HOMO-LUMO transition for the ground state as it has been explained in recent publications [56–58].

The results for the calculation of the maximum absorption wavelength of the DACC molecule in the presence of chloroform following the three methodologies presented in the previous paragraph are shown in Table 2.

Table 2: Maximum absorption wavelength of the DACC molecule in nm calculated according to the three methodologies explained in the text: LR (Linear Response calculation), SS (Solvent-specific two-part calculation) and HL (based on the HOMO-LUMO transition fro the ground state)

.

Density Functional	LR	SS	HL
B3LYP	290	310	258
BLYP	382	426	419
PBE0	266	274	225
PBEPBE	347	376	375
CAM-B3LYP	247	248	158
M11	238	237	127
M11L	301	328	323
MN12L	276	298	294
MN12SX	262	271	253
N12	328	358	354
N12SX	268	278	259
HSEH1PBE	271	282	263
ωB97XD	246	246	136

It can be concluded from the examination of Table 2 that the PBEPBE density functional is the best for the prediction of the maximum absorption wavelength of DACC in chloroform if a LR calculation is considered. For the case of a SS calculation, this functional does not behave quite well and now the best density functional is N12 which also behaves remakably well considering the approximate HL methodology. Thus, the N12 density functional will be chosen for the calculation of the Conceptual DFT descriptors that will give us an idea of the chemical reactivity of the molecule under study.

By considering the already mentioned KID procedure together with an approximation by finite differences, the global reactivity descriptors related to Conceptual DFT can be expressed through different formulas: the Electronegativity χ is equal to $-\frac{1}{2}(I+A) \approx \frac{1}{2}(\epsilon_L + \epsilon_H)$ [9, 10], while the Global Hardness η is equal to $(I-A) \approx (\epsilon_L - \epsilon_H)$ [9, 10], the Electrophilicity ω is related to $\mu^2 / 2\eta = (I+A)^2 / 4(I-A) \approx (\epsilon_L + \epsilon_H)^2 / 4(\epsilon_L - \epsilon_H)$ [59]. The other group of global reactivity descriptors is constituted by the Electrodonating Power ω^- = $(3I+A)^2 / 16(I-A) \approx (3\epsilon_H + \epsilon_L)^2 / 16\eta$ [60], the Electroaccepting Power ω^+ = $(I+3A)^2 / 16(I-A) \approx (\epsilon_H + 3\epsilon_L)^2 / 16\eta$ [60] and the Net Electrophilicity $\Delta\omega^{\pm} = \omega^+ - (-\omega^-) = \omega^+ + \omega^-$ [61]. In these expressions, ϵ_H and ϵ_L are the energies of the HOMO and LUMO, respectively.

On the basis of the previous comments, the results for the HOMO and LUMO energies calculated with the N12 density functional will be adequate for predicting the values of the global reactivity descriptors and these are presented in Table 3 for the electronegativity χ, chemical hardness η, global electrophilicity ω, electroaccepting (ω^+) and electrodonating (ω^-) powers as well as the net electrophilicity.

Table 3: Global reactivity descriptors for the DACC molecule calculated with the N12 density functional and the Def2TZVP basis set using chloroform as the solvent according to the SMD solvation model.

Electronegativity (χ)	Chemical Hardness (η)	Electrophilicity (ω)
4.1923	3.6705	2.3941
Electrodonating	Electroaccepting	Net Electrophilicity
Power (ω^-)	Power (ω^+)	($\Delta\omega^{\pm}$)
7.1138	2.9215	10.0354

One way of complementing the results of the calculation of the global reactivity descriptors is by considering an analysis of the molecular electrostatic potential (MEP) which is well-established method to give the reactive properties of a wide variety of chemical systems in both electrophilic and nucleophilic reactions. The electrophilic reactivity is related to the negative regions of the MEP which are usually colored as red, orange or yellow. In turn, the surfaces colored in green or blue denote positive regions that will be prone to nucleophilic attack. The representation of the MEP for the DACC molecule considered in this study is displayed in Figure 4:

Figure 4: Molecular Electrostatic Potential of the DACC molecule showing the the negative regions colored in yellow and the negative regions colored in blue

If we consider the previous mentioned ideas, the definitions for the local reactivity descriptors will be: Nucleophilic Fukui Function $f^+(\mathbf{r}) = \rho_{N+1}(\mathbf{r}) - \rho_N(\mathbf{r})$ [9, 10], Electrophilic Fukui Function $f^-(\mathbf{r}) = \rho_N(\mathbf{r}) - \rho_{N-1}(\mathbf{r})$ [9, 10] and Dual Descriptor $\Delta f(\mathbf{r}) = (\partial f(\mathbf{r}) / \partial N)_{v(\mathbf{r})}$ [62–67], while the Nucleophilic Parr Function $P^-(\mathbf{r})$ will be equal to $\rho_s^{rc}(\mathbf{r})$ and the Electrophilic Parr Function $P^+(\mathbf{r})$ will be equal to $\rho_s^{ra}(\mathbf{r})$ [68, 69]. It must be remarked that $\rho_{N+1}(\mathbf{r})$, $\rho_N(\mathbf{r})$, and $\rho_{N-1}(\mathbf{r})$ are the electronic densities at point $\mathbf{r}$ for a system with $N+1$, N, and $N-1$ electrons, respectively, and $\rho_s^{rc}(\mathbf{r})$ and $\rho_s^{ra}(\mathbf{r})$ are related to the atomic spin density (ASD) at the $\mathbf{r}$ atom of the radical cation or anion of a given molecule, respectively [70].

The electrophilic and nucleophilic Fukui functions of the DACC molecule are displayed in Figure 5:

Figure 5: Graphical representation of the Electrophilic Fukui function $f^{-}(\mathbf{r})$ (left) and Nucleophilic Fukui function $f^{+}(\mathbf{r})$ (right) of the DACC molecule

In a fascinating ongoing work by Martínez-Araya [67], it has been demonstrated that while the Fukui work is an excellent descriptor to comprehend the local reactivity of the molecules, the Δf_k will perform better for the prediction of the preferred sites for the electrophilic and nucleophilic attacks.. Consequently, it has been chosen to display the outcomes for the Condensed Dual Descriptor Δf_k as computed from either Mulliken Population Analysis (M) or Natural Population Analysis (N) in correlation with the Nucleophilic Parr Function P_k^+ and Electrophilic Parr Function P_k^- proposed by Domingo et al [68, 69] considering atomic spin densities originating from the specified Mulliken Population Analysis (M) or from the Hirshfeld Population Analysis (H).

Table 4 displays the results for the calculation of these local reactivity descriptors for the DACC molecule in relation with the structure shown in Figure 6. It must be noted that the only results presented here are for those atomic sites where the Δf_k (which is itself multiplied by 100) are greater than 2. Also, the H atoms are not shown.

Figure 6: Molecular structure of DACC showing the type and numbering of the atoms

Table 4: Local reactivity descriptors for the DACC molecule calculated as mentioned in the text where M stands for Mulliken Population Analysis, N corresponds to Natural Population Analysis and H means Hirshfeld Population Analysis

Atom	Δf_k (M)	Δf_k (N)	P_k^+ (M)	P_k^- (M)	P_k^+ (H)	P_k^- (H)
1 Br	21.84	8.32	0.1875	0.0961	0.1915	0.0893
2 Br	10.89	4.57	0.1309	0.0962	0.1348	0.0890
3 Cl	-3.56	-2.38	0.0077	0.0124	0.0112	0.0120
4 O	-7.05	-3.67	0.0091	0.0539	0.0108	0.0492
5 N	-19.31	-6.67	0.0120	0.1481	0.0087	0.1358
6 C	16.05	1.61	0.1165	0.0044	0.1121	0.0056
7 C	7.80	0.17	0.0542	0.0098	0.1121	0.0067
10 C	-11.64	-2.57	0.0530	0.1256	0.0685	0.1143
14 C	-6.42	-2.31	0.0091	0.0000	0.0478	0.0115
16 C	-14.79	-4.44	0.0156	0.1250	0.0051	0.1067
18 C	2.39	2.20	0.0668	0.0486	0.0516	0.0444
19 C	3.52	1.86	0.0930	0.0095	0.0709	0.0536

After inspection of Table 4, it can be concluded that the sites for electrophilic attack will be N5 and to a lesser extent C10 and C14, while the reactive places for nucleophilic attack will be located over Br1, Br2 and C6.

While thinking about a given molecular species as a potential therapeutic medication, it is standard to check if the considered species pursues the Lipinsky Rule of Five which is utilized to foresee whether a compound has or not has a drug-like character [71]. The molecular properties that are related to the drug-like character have been predicted by using MolSoft and Molinspiration software and are presented in Table 5 where miLogP represents the octanol/water partition coefficient, TPSA is the molecular polar surface area, natoms is the number of atoms of the molecule, nON and nOHNH are the number of hydrogen bond acceptors and hydrogen bond donors respectively, nviol is the number

of violations of the Lipinsky Rule of Five, nrotb is the number of rotatable bonds, volume is the molecular volume, and MW is the molecular weight of the studied system.

Table 5: Molecular properties of the DACC molecule calculated to verify the Lipinsky Rule of Five

Molecule	miLogP	TPSA	nAtoms	nON	nOHNH	nviol	nrotb	volume	MW
DACC	5.36	20.31	20	2	0	1	0	259.34	415.51

An alternate methodology can be trailed by considering similarity seeks in the chemical space of molecules with structures that can be contrasted with those that are being contemplated possessing known pharmacological properties.

As has been specified in the Settings and Computational Methods section, this assignment can be performed utilizing the online Molinspiration programming for the forecast of the bioactivity score for various drug targets (GPCR ligands, Kinase inhibitors, Ion channel modulators, Enzymes and Nuclear receptors). The outcomes are named Bioactivity Scores and their values for the DACC are displayed in Table 6.

Table 6: Reactivity scores of the DACC molecule calculated on the basis of GPCR Ligand, Ion Channel Modulator, Nuclear Receptor Ligand, Kinase Inhibitor, Protease Inhibitor and Enzyme Inhibitor interactions

Molecule	GPCR Ligand	Ion Channel Modulator	Kinase Inhibitor	Nuclear Receptor Ligand	Protease Inhibitor	Enzyme Inhibitor
DACC	-0.23	-0.20	0.22	-0.24	-0.22	-0.15

The interpretation given to these bioactivity scores are that a specific molecular system is active when the bioactivity score is greater than 0, it is moderately active when the bioactivity score lies between -5.0 and 0.0, and will be inactive is the bioactivity score is lower than -5.0. Thus, DACC was found to be moderately bioactive towards all the enzymes considered for the study with the exception of the Kinase Inhibition for which case the DACC molecule may be considered as active. This represents a confirmation of the presumed bioactivity of this molecule.

Conclusions

A new and original route of synthesis of an azepin-derivative, which has been called with acronym DACC, with potential therapeutic abilities has been presented in this paper. The structure of the new compound has been characterized by means of diverse spectroscopic techniques.

Moreover, a study was performed on the chemical reactivity of the DACC molecules based on the Conceptual DFT as a tool for rationalizing the interaction between different molecular systems.

The knowledge of the values of the global and local descriptors of the molecular reactivity of the DACC molecule studied could be useful in the development of new drugs based on this compound or some analogs.

The information of the estimations of the global and local reactivity descriptors of the DACC species considered could be valuable in the advancement of the design of new medications based on the structure of this and analog compounds.

At last, the molecular properties identified with the bioavailability have been anticipated utilizing diverse procedures already portrayed in the specialized literature, and the descriptors utilized for the evaluation of the bioactivity permitted to describe the DACC molecule as being bioactive towards the Kinase Inhibitor considered in the study.

Acknowledgements

KSP gratefully thank the Directors of Central Instrumentation Facility (CIF), Innovation Centre, MAHE and Manipal Centre for Natural Sciences, MAHE for analytical facilities and financial

support, respectively. DGM is a research of CIMAV and CONACYT and conducted a part of this research while a Visiting Professorship at the Universitat de les Illes Balears from which support is gratefully acknowledged. This work was cofunded by the Ministerio de Economía y Competitividad (MINECO) and the European Fund for Regional Development (FEDER) (CTQ2014-55835-R).

References

[1] A. F. Ambrósio, P. Soares-da Silva, C. M. Carvalho, A. P. Carvalho, Mechanisms of Action of Carbamazepine and Its Derivatives, Oxcarbazepine, BIA 2-093, and BIA 2-024, Neurochemical Research 27 (1/2) (2002) 121–130.

[2] P. K. Gillman, Tricyclic Antidepressant Pharmacology and Therapeutic Drug Interactions Updated, British Journal of Pharmacology 151 (6) (2007) 737–748.

[3] D. A. Ciraulo, R. I. Shader, D. J. Greenblatt, Clinical Pharmacology and Therapeuticsof Antidepressants, in: Pharmacotherapy of Depression, Humana Press, Totowa, NJ, 2010, pp. 33–124.

[4] D. W. Nelson, Dibenzazepine-Based Sodium Channel Blockers for the Treatment of Neuropathic Pain, Wiley-Blackwell, 2013, Ch. 8, pp. 115–133.

[5] X. Zhang, Y. Yang, Y. Liang, Palladium-Catalyzed Double N-Arylation to Synthesize Multisubstituted Dibenzoazepine Derivatives, Tetrahedron Letters 53 (47) (2012) 6406–6408.

[6] K. S. Prasad, R. A. Costa, A. D. S. Branches, K. M. T. Oliveira, Novel Route for the Synthesis of Azepine Derivative Using Tin-Based Catalyst: Spectroscopic Characterization and Theoretical Investigations, Journal of Molecular Structure 1178 (2019) 491–499.

[7] E. Rekka, P. Kourounakis, Chemistry and Molecular Aspects of Drug Design and Action, CRC Press, Boca Raton, 2008.

[8] G. Náray-Szabó, A. Warshel, Computational Approaches to Biochemical Reactivity, Kluwer Academic Publishers, New York, 2002.

[9] R. Parr, W. Yang, Density-Functional Theory of Atoms and Molecules, Oxford University Press, New York, 1989.

[10] P. Geerlings, F. De Proft, W. Langenaeker, Conceptual Density Functional Theory, Chemical Reviews 103 (2003) 1793–1873.

[11] J. Gázquez, Perspectives on the Density Functional Theory of Chemical Reactivity, Journal of the Mexican Chemical Society 52 (1) (2008) 3–10.

[12] H. Chermette, Density Functional Theory: A Powerful Tool for Theoretical Studies in Coordination Chemistry, Coordination Chemical Reviews 178-180 (1998) 699–721.

[13] P. Goszczycki, K. Stadnicka, M. Z. Brela, J. Grolik, K. Ostrowska, Synthesis, Crystal Structures, and Optical Properties of the π-π Interacting Pyrrolo[2,3-B]Quinoxaline Derivatives Containing 2-Thienyl Substituent, Journal of Molecular Structure 1146 (2017) 337–346.

[14] V. V. Menon, E. Fazal, Y. S. Mary, C. Y. Panicker, S. Armaković, S. J. Armaković, S. Nagarajan, C. Van Alsenoy, FT-IR, FT-Raman and NMR Characterization of 2-Isopropyl-5-Methylcyclohexyl Quinoline-2-Carboxylate and Investigation of Its Reactive and Optoelectronic Properties by Molecular Dynamics Simulations and DFT Calculations, Journal of Molecular Structure 1127 (C) (2017) 124–137.

[15] G. K. Gupta, V. Kumar, Chemical Drug Design, Walter de Gruyter GmbH, Berlin, 2016.

[16] M. Gore, U. B. Jagtap, Computational Drug Discovery and Design, Springer Science+Business Media, LLC, New York, 2018.

[17] T. A. Halgren, Merck Molecular Force Field. I. Basis, Form, Scope, Parameterization, and Performance of MMFF94, Journal of Computational Chemistry 17 (5-6) (1996) 490–519.

[18] T. A. Halgren, Merck Molecular Force Field. II. MMFF94 van der Waals and Electrostatic Parameters for Intermolecular Interactions, Journal of Computational Chemistry 17 (5-6) (1996) 520–552.

[19] T. A. Halgren, MMFF VI. MMFF94s Option for Energy Minimization Studies, Journal of Computational Chemistry 20 (7) (1999) 720–729.

[20] T. A. Halgren, R. B. Nachbar, Merck Molecular Force Field. IV. Conformational Energies and Geometries for MMFF94, Journal of Computational Chemistry 17 (5-6) (1996) 587–615.

[21] T. A. Halgren, Merck Molecular Force field. V. Extension of MMFF94 Using Experimental Data, Additional Computational Data, and Empirical Rules, Journal of Computational Chemistry 17 (5-6) (1996) 616–641.

[22] J. Frau, D. Glossman-Mitnik, Molecular Reactivity and Absorption Properties of Melanoidin Blue-G1 through Conceptual DFT, Molecules 23 (3) (2018) 559–15.

[23] J. Frau, D. Glossman-Mitnik, Conceptual DFT Study of the Local Chemical Reactivity of the Dilysyldipyrrolones A and B Intermediate Melanoidins, Theoretical Chemistry Accounts 137 (5) (2018) 1210.

[24] J. Frau, D. Glossman-Mitnik, Conceptual DFT Study of the Local Chemical Reactivity of the Colored BISARG Melanoidin and Its Protonated Derivative, Frontiers in Chemistry 6 (136) (2018) 1–9.

[25] J. Frau, D. Glossman-Mitnik, Molecular Reactivity of some Maillard Reaction Products Studied through Conceptual DFT, ContemporaryChemistry 1 (1) (2018) 1–14.

[26] J. Frau, D. Glossman-Mitnik, Computational Study of the Chemical Reactivity of the Blue-M1 Intermediate Melanoidin, Computational and Theoretical Chemistry 1134 (2018) 22–29.

[27] J. Frau, D. Glossman-Mitnik, Chemical Reactivity Theory Applied to the Calculation of the Local Reactivity Descriptors of a Colored Maillard Reaction Product, Chemical Science International Journal 22 (4) (2018) 1–14.

[28] J. Frau, D. Glossman-Mitnik, Blue M2: An Intermediate Melanoidin Studied via Conceptual DFT, Journal of Molecular Modeling 24 (138) (2018) 1–13.

[29] J. Frau, N. Flores-Holguín, D. Glossman-Mitnik, Chemical Reactivity Properties, pKa Values, AGEs Inhibitor Abilities and Bioactivity Scores of the Mirabamides A–H Peptides of Marine Origin Studied by Means of Conceptual DFT, Marine Drugs 16 (9) (2018) 302–19.

[30] M. J. Frisch, G. W. Trucks, H. B. Schlegel, G. E. Scuseria, M. A. Robb, J. R. Cheeseman, G. Scalmani, V. Barone, B. Mennucci, G. A. Petersson, H. Nakatsuji, M. Caricato, X. Li, H. P. Hratchian, A. F. Izmaylov, J. Bloino, G. Zheng, J. L. Sonnenberg, M. Hada, M. Ehara, K. Toyota, R. Fukuda, J. Hasegawa, M. Ishida, T. Nakajima, Y. Honda, O. Kitao, H. Nakai, T. Vreven, J. A. Montgomery, Jr., J. E. Peralta, F. Ogliaro, M. Bearpark, J. J. Heyd, E. Brothers, K. N. Kudin, V. N. Staroverov, R. Kobayashi, J. Normand, K. Raghavachari, A. Rendell, J. C. Burant, S. S. Iyengar, J. Tomasi, M. Cossi, N. Rega, J. M. Millam, M. Klene, J. E. Knox, J. B. Cross, V. Bakken, C. Adamo, J. Jaramillo, R. Gomperts, R. E. Stratmann, O. Yazyev, A. J. Austin, R. Cammi, C. Pomelli, J. W. Ochterski, R. L. Martin, K. Morokuma, V. G. Zakrzewski, G. A. Voth, P. Salvador, J. J. Dannenberg, S. Dapprich, A. D. Daniels, O. Farkas, J. B. Foresman, J. V. Ortiz, J. Cioslowski, D. J. Fox, Gaussian 09 Revision E.01, Gaussian Inc., Wallingford CT, 2016 (2016).

[31] F. Weigend, R. Ahlrichs, Balanced Basis Sets of Split Valence, Triple Zeta Valence and Quadruple Zeta Valence Quality for H to Rn: Design and Assessment of Accuracy, Physical Chemistry Chemical Physics 7 (2005) 3297–3305.

[32] F. Weigend, Accurate Coulomb-fitting Basis Sets for H to R, Physical Chemistry Chemical Physics 8 (2006) 1057–1065.

[33] A. Marenich, C. Cramer, D. Truhlar, Universal Solvation Model Based on Solute Electron Density and a Continuum Model of the Solvent Defined by the Bulk Dielectric Constant and Atomic Surface Tensions, Journal of Physical Chemistry B 113 (2009) 6378–6396.

[34] A. Becke, Density-Functional Thermochemistry. III. The Role of Exact Exchange, Journal of Chemical Physics 98 (1993) 5648–5652.

[35] A. Becke, Density-Functional Exchange-Energy Approximation with Correct Asymptotic-Behavior, Physical Review A 38 (1988) 3098–3100.

[36] C. Lee, W. Yang, R. Parr, Development of the Colle-Salvetti Correlation-Energy Formula into a Functional of the Electron Density, Physical Review B 37 (1988) 785–789.

[37] C. Adamo, V. Barone, Toward Reliable Density Functional Methods without Adjustable Parameters: The PBE0 Model, Chemical Physics 110 (1999) 6158–6169.

[38] J. Perdew, K. Burke, M. Ernzerhof, Generalized Gradient Approximation Made Simple, Physical Review Letters 77 (18) (1996) 3865–3868.

[39] J. Perdew, K. Burke, M. Ersernhof, Erratum: Generalized Gradient Approximation Made Simple, Physical Review Letters 78 (1997) 1396.

[40] T. Yanai, D. P. Tew, N. C. Handy, A New Hybrid Exchange-Correlation Functional Using the Coulomb-Attenuating Method (CAM-B3LYP), Chemical Physics Letters 393 (1-3) (2004) 51–57.

[41] R. Peverati, D. G. Truhlar, Improving the Accuracy of Hybrid Meta-GGA Density Functionals by Range Separation, The Journal of Physical Chemistry Letters 2 (21) (2011) 2810–2817.

[42] R. Peverati, D. G. Truhlar, M11-L: A Local Density Functional That Provides Improved Accuracy for Electronic Structure Calculations in Chemistry and Physics, The Journal of Physical Chemistry Letters 3 (1) (2012) 117–124.

[43] R. Peverati, D. G. Truhlar, An Improved and Broadly Accurate Local Approximation to the Exchange-Correlation Density Functional: the MN12-L Functional for Electronic Structure Calculations in Chemistry and Physics, Physical Chemistry Chemical Physics 14 (38) (2012) 13171–13174.

[44] R. Peverati, D. G. Truhlar, Screened-Exchange Density Functionals with Broad Accuracy for Chemistry and Solid-State Physics, Physical Chemistry Chemical Physics 14 (47) (2012) 16187–16191.

[45] R. Peverati, D. G. Truhlar, Exchange-Correlation Functional with Good Accuracy for Both Structural and Energetic Properties while Depending Only on the Density and Its Gradient., Journal of Chemical Theory and Computation 8 (7) (2012) 2310–2319.

[46] J. Heyd, G. Scuseria, Efficient Hybrid Density Functional Calculations in Solids: Assessment of the Heyd-Scuseria-Ernzerhof Screened Coulomb Hybrid Functional, The Journal of Chemical Physics 121 (3) (2004) 1187–1192.

[47] J. Heyd, G. E. Scuseria, Assessment and Validation of a Screened Coulomb Hybrid Density Functional, The Journal of Chemical Physics 120 (16) (2004) 7274–7280.

[48] J. Heyd, J. E. Peralta, G. E. Scuseria, R. L. Martin, Energy Band Gaps and Lattice Parameters Evaluated with the Heyd-Scuseria-Ernzerhof Screened Hybrid Functional, The Journal of Chemical Physics 123 (17) (2005) 174101.

[49] J. Heyd, G. E. Scuseria, M. Ernzerhof, Erratum: Hybrid Functionals Based on a Screened Coulomb Potential [J. Chem. Phys. 118, 8207 (2003)], The Journal of Chemical Physics 124 (21) (2006) 219906.

[50] T. M. Henderson, A. F. Izmaylov, G. Scalmani, G. E. Scuseria, Can Short-Range Hybrids Describe Long-Range-Dependent Properties?, The Journal of Chemical Physics 131 (4) (2009) 044108.

[51] A. F. Izmaylov, G. E. Scuseria, M. J. Frisch, Efficient Evaluation of Short-Range Hartree-Fock Exchange in Large Molecules and Periodic Systems, The Journal of Chemical Physics 125 (10) (2006) 104103.

[52] A. V. Krukau, O. A. Vydrov, A. F. Izmaylov, G. E. Scuseria, Influence of the Exchange Screening Parameter on the Performance of Screened Hybrid Functionals, The Journal of Chemical Physics 125 (22) (2006) 224106.

[53] J. Chai, M. Head-Gordon, Long-Range Corrected Hybrid Density Functionals with Damped Atom-Atom Dispersion Corrections, Physical Chemistry Chemical Physics 10 (2008) 6615–6620.

[54] H. Singh, N. Gupta, P. Kumar, S. K. Dubey, P. K. Sharma, A New Industrial Process for 10-Methoxyiminostilbene: Key Intermediate for the Synthesis of Oxcarbazepine, Organic Process Research & Development 13 (5) (2009) 870–874.

[55] J. Foresman, A. Frisch, Exploring Chemistry with Electronic Structure Methods - Third Edition, Gaussian, Inc., Wallingford, CT, 2015.

[56] A. D. Becke, Vertical Excitation Energies From the Adiabatic Connection, The Journal of Chemical Physics 145 (19) (2016) 194107.

[57] E. J. Baerends, O. V. Gritsenko, R. van Meer, The Kohn-Sham Gap, the Fundamental Gap and the Optical Gap: The Physical Meaning of Occupied and Virtual Kohn-Sham Orbital Energies, Physical Chemistry Chemical Physics 15 (39) (2013) 16408–16425.

[58] R. van Meer, O. V. Gritsenko, E. J. Baerends, Physical Meaning of Virtual Kohn-Sham Orbitals and Orbital Energies: An Ideal Basis for the Description of Molecular Excitations, Journal of Chemical Theory and Computation 10 (10) (2014) 4432–4441.

[59] R. Parr, L. Szentpaly, S. Liu, Electrophilicity Index, Journal of the American Chemical Societ 121 (1999) 1922–1924.

[60] J. Gázquez, A. Cedillo, A. Vela, Electrodonating and Electroaccepting Powers, Journal of Physical Chemistry A 111 (10) (2007) 1966–1970.

[61] P. Chattaraj, A. Chakraborty, S. Giri, Net Electrophilicity, Journal of Physical Chemistry A 113 (37) (2009) 10068–10074.

[62] A. Toro-Labbé (Ed.), Theoretical Aspects of Chemical Reactivity, Elsevier Science, Amsterdam, 2007.

[63] C. Morell, A. Grand, A. Toro-Labbé, New Dual Descriptor for Chemical Reactivity, Journal of Physical Chemistry A 109 (2005) 205–212.

[64] C. Morell, A. Grand, A. Toro-Labbé, Theoretical Support for Using the $\Delta f(\mathbf{r})$ Descriptor, Chemical Physics Letters 425 (2006) 342–346.

[65] J. I. Martínez-Araya, Revisiting Caffeate's Capabilities as a Complexation Agent to Silver Cation in Mining Processes by means of the Dual Descriptor – A Conceptual DFT Approach, Journal of Molecular Modeling 18 (2012) 4299–4307.

[66] J. I. Martínez-Araya, Explaining Reaction Mechanisms Using the Dual Descriptor: A Complementary Tool to the Molecular Electrostatic Potential, Journal of Molecular Modeling 19 (7) (2012) 2715–2722.

[67] J. I. Martínez-Araya, Why is the Dual Descriptor a More Accurate Local Reactivity Descriptor than Fukui Functions?, Journal of Mathematical Chemistry 53 (2) (2015) 451–465.

[68] L. R. Domingo, P. Pérez, J. Sáez, Understanding the Local Reactivity in Polar Organic Reactions through Electrophilic and Nucleophilic Parr Functions, RSC Advances 3 (2013) 1486–1494.

[69] E. Chamorro, P. Pérez, L. R. Domingo, On the Nature of Parr Functions to Predict the Most Reactive Sites along Organic Polar Reactions, Chemical Physics Letters 582 (2013) 141–143.

[70] L. R. Domingo, M. Ríos-Gutiérrez, P. Pérez, Applications of the Conceptual Density Functional Theory Indices to Organic Chemistry Reactivity, Molecules 21 (2016) 748.

[71] P. Leeson, Drug Discovery: Chemical Beauty Contest, Nature 481 (7382) (2012) 455–456.

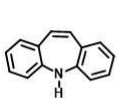

1

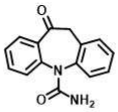

2

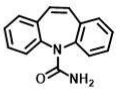

3

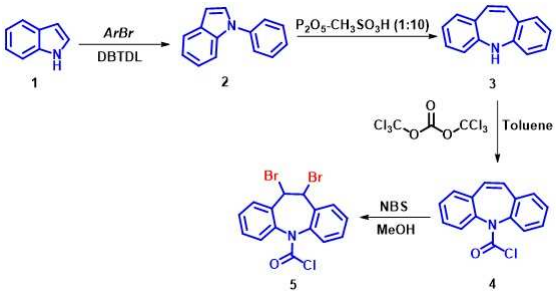

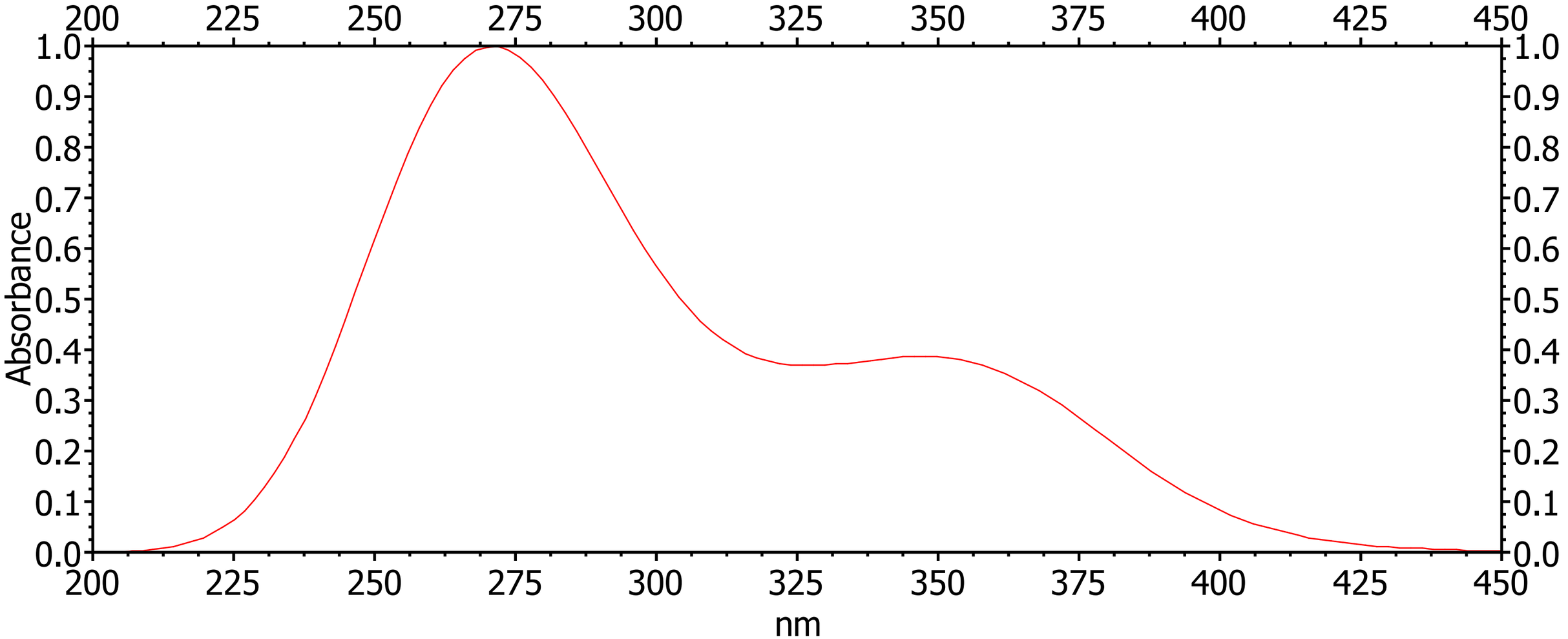
200
225
250
275
300
325
350
375
400
425
450
1.0
0.9
0.8
0.7
0.6
0.5
0.4
0.3
0.2
0.1
0.0
Absorbance
nm

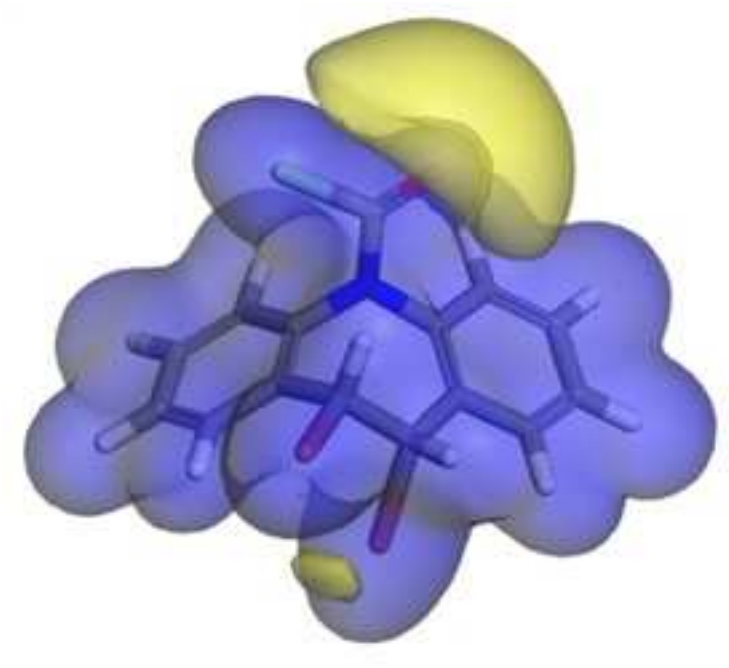

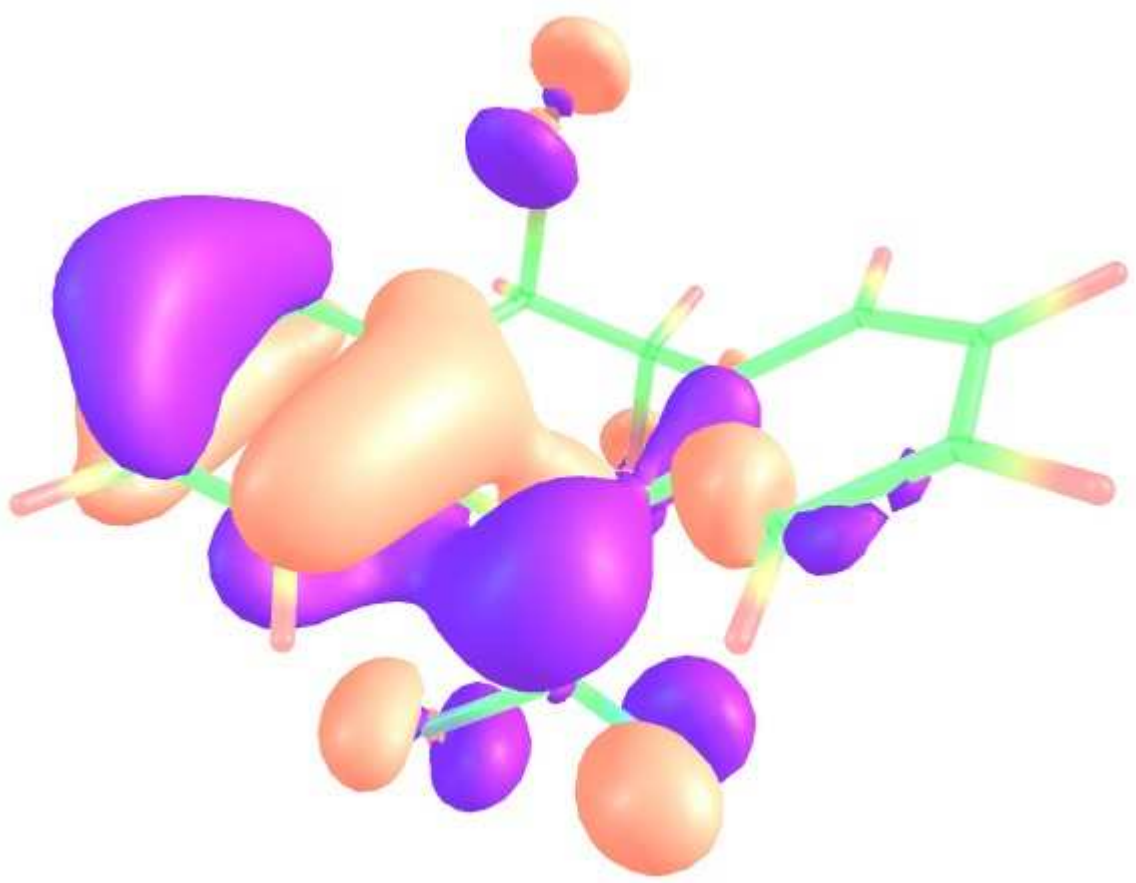

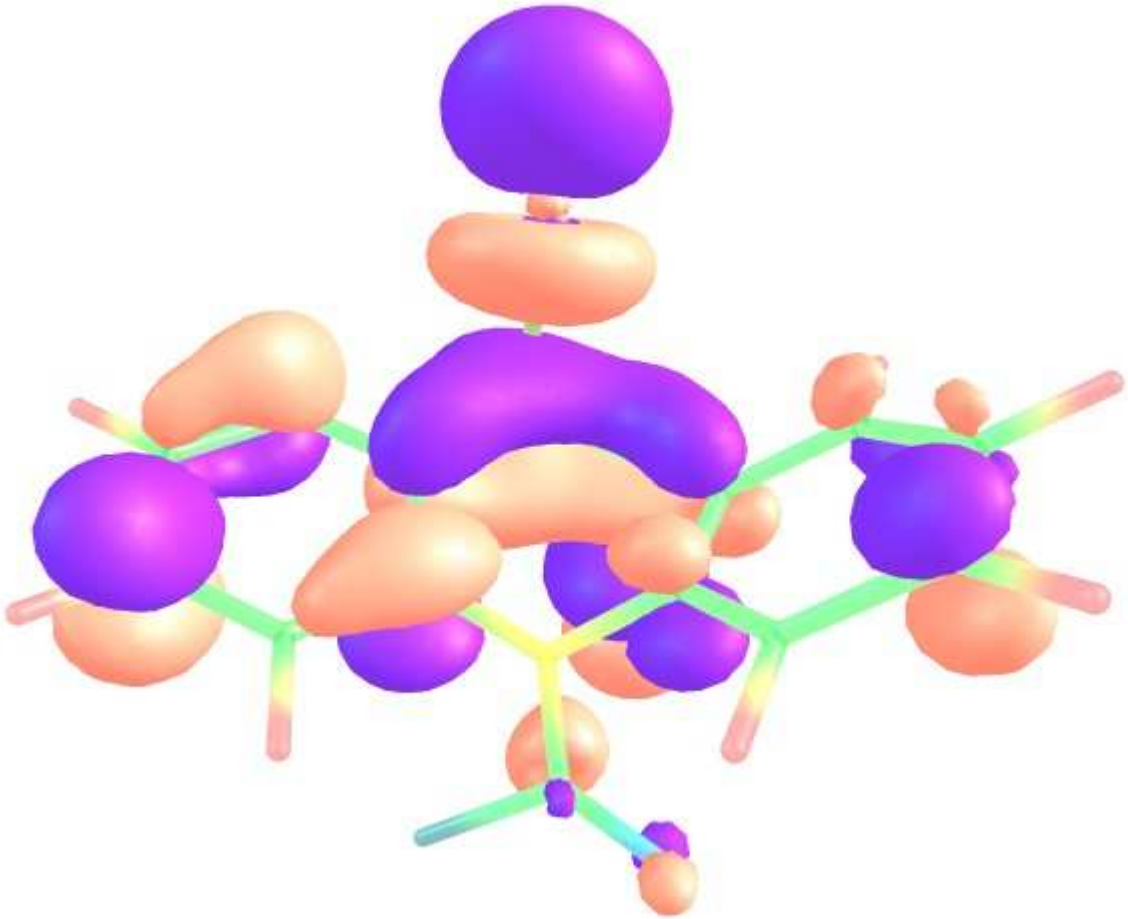

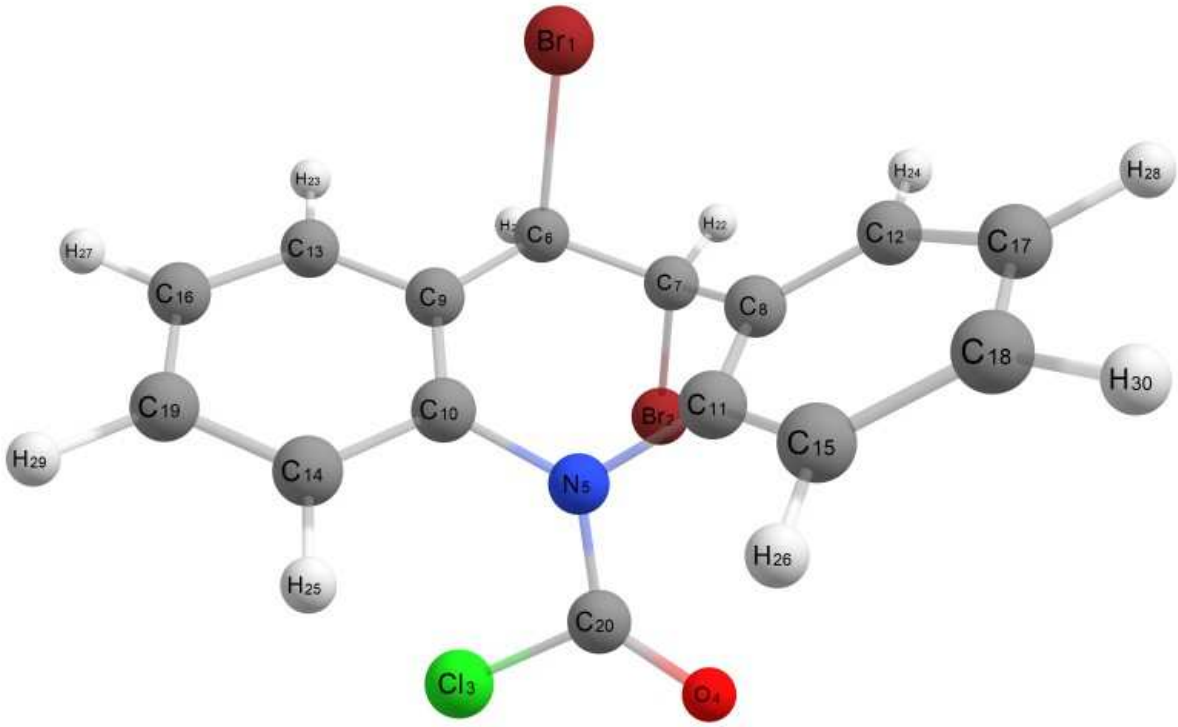

Highlights

- Synthesis of 10,11-Dibromo-10,11-dihydro-5H-dibenzo[b,f]azepine-5-carbonyl chloride.
- HOMO-LUMO energy values are used in predicting global reactivity descriptors.
- The electrophilic and nucleophilic Fukui functions were determined.
- Title molecule being more bioactive towards Kinase Inhibitor than with other enzymes.